

RESEARCH

Open Access



# The role of proteasome in muscle wasting of experimental arthritis

Vivian Oliveira Nunes Teixeira<sup>1,2</sup>, Bárbara Jonson Bartikoski<sup>1,2</sup>, Rafaela Cavalheiro do Espirito Santo<sup>1,2\*</sup> , Paulo Vinícius Gil Alabarse<sup>1,2,6</sup>, Khetam Ghannan<sup>3</sup>, Jordana Miranda Souza Silva<sup>1,2</sup>, Lidiane Isabel Filippin<sup>2,4</sup>, Fernanda Visioli<sup>5</sup>, Lorena Martinez-Gamboa<sup>3</sup>, Eugen Feist<sup>3</sup> and Ricardo Machado Xavier<sup>1,2</sup>

## Abstract

**Background** Rheumatoid arthritis is an autoimmune inflammatory disease that often leads patients to muscle impairment and physical disability. This study aimed to evaluate changes in the activity of proteasome system in skeletal muscles of mice with collagen-induced arthritis (CIA) and treated with etanercept or methotrexate.

**Methods** Male DBA1/J mice were divided into four groups (n = 8 each): CIA-Vehicle (treated with saline), CIA-ETN (treated with etanercept, 5.5 mg/kg), CIA-MTX (treated with methotrexate, 35 mg/kg) and CO (healthy control group). Mice were treated two times a week for 6 weeks. Clinical score and hind paw edema were measured. Muscles were weighted after euthanasia and used to quantify proteasome activity, gene (MuRF-1, PMS $\alpha$ 4, PSM $\beta$ 5, PSM $\beta$ 6, PSM $\beta$ 7, PSM $\beta$ 8, PSM $\beta$ 9, and PSM $\beta$ 10), and protein (PSM $\beta$ 1, PSM $\beta$ 5, PSM $\beta$ 11, PSM $\beta$ 5i) expression of proteasome subunits.

**Results** Both treatments slowed disease development, but only CIA-ETN maintained muscle weight compared to CIA-MTX and CIA-Vehicle groups. Etanercept treatment showed caspase-like activity of 26S proteasome similar to CO group, while CIA-Vehicle and CIA-MTX had higher activity compared to CO group ( $p$ : 0.0057). MuRF-1 mRNA expression was decreased after etanercept administration compared to CIA-Vehicle and CO groups ( $p$ : 0.002,  $p$ : 0.007, respectively). PSM $\beta$ 8 and PSM $\beta$ 9 mRNA levels were increased in CIA-Vehicle and CIA-MTX compared to CO group, while CIA-ETN presented no difference from CO. PMS $\beta$ 6 mRNA expression was higher in CIA-Vehicle and CIA-MTX groups than in CO group. Protein levels of the PSM $\beta$ 5 subunit were increased in CO group compared to CIA-Vehicle; after both etanercept and methotrexate treatments, PSM $\beta$ 5 expression was higher than in CIA-Vehicle group and did not differ from CO group expression ( $p$ : 0.0025,  $p$ : 0.001, respectively). The inflammation-induced subunit  $\beta$ 1 (LMP2) was enhanced after methotrexate treatment compared to CO group ( $p$ : 0.043).

**Conclusions** The results of CIA-Vehicle show that arthritis increases muscle proteasome activation by enhanced caspase-like activity of 26S proteasome and increased PSM $\beta$ 8 and PSM $\beta$ 9 mRNA levels. Etanercept treatment was able to maintain the muscle weight and to modulate proteasome so that its activity and gene expression were compared to CO after TNF inhibition. The protein expression of inflammation-induced proteasome subunit was increased in muscle of CIA-MTX group but not following etanercept treatment. Thus, anti-TNF treatment may be an interesting approach to attenuate the arthritis-related muscle wasting.

**Keywords** Experimental arthritis, Muscle wasting, Proteasome, TNF inhibitor

\*Correspondence:

Rafaela Cavalheiro do Espirito Santo  
rcsanto@hcpa.edu.br

Full list of author information is available at the end of the article



© The Author(s) 2023. **Open Access** This article is licensed under a Creative Commons Attribution 4.0 International License, which permits use, sharing, adaptation, distribution and reproduction in any medium or format, as long as you give appropriate credit to the original author(s) and the source, provide a link to the Creative Commons licence, and indicate if changes were made. The images or other third party material in this article are included in the article's Creative Commons licence, unless indicated otherwise in a credit line to the material. If material is not included in the article's Creative Commons licence and your intended use is not permitted by statutory regulation or exceeds the permitted use, you will need to obtain permission directly from the copyright holder. To view a copy of this licence, visit <http://creativecommons.org/licenses/by/4.0/>.

## Background

Rheumatoid arthritis (RA) is an inflammatory systemic autoimmune disease with persistent polyarticular synovitis that can progress to joint destruction [1]. Also, systemic complications are associated with RA, including significant muscle wasting [2, 3]. The triggering mechanisms for muscle wasting in RA are not fully elucidated, but the causes are likely to be hormone dysfunction (insulin resistance and enhanced myostatin) and cytokine-driven hypercatabolism, with particular involvement of the pro-inflammatory cytokine tumor necrosis factor (TNF) [4, 5]. Muscle wasting is associated with severe tissue protein breakdown involving different proteolytic pathways, such as the ubiquitin–proteasome system, which seems to have an important role in RA muscle loss [6–8].

The ubiquitin–proteasome system is a major pathway directly or indirectly involved in several catabolic conditions and may be linked to higher pro-inflammatory content [9]. The proteasome is a protein complex and its different components can be named according to structure and activity. The core structure of the proteasome is referred to as 20S, and the extremities are called 19S. The combination of 20S and 19S forms the 26S proteasome [10]. The 20S proteasome is cylinder-shaped and contains four rings with multiple subunits and protease activity in the inner cavity. The rings are made of seven  $\alpha$  subunits and seven  $\beta$  subunits [11]. Only the  $\beta 5$  (Psm5),  $\beta 1$  (Psm6), and  $\beta 2$  (Psm7) subunits have protease activities [10, 12]. Each subunit represents a distinct catalytic activity in the proteasome: chymotrypsin-like, peptidyl-glutamyl peptide-hydrolyzing (caspase-like), and trypsin-like. When the 20S core attaches to its regulatory enzyme (19S), it recognizes and breaks denatured ubiquitinated proteins in an ATP-dependent fashion [13]. Another regulator complex is the 11S (or PA 28), which can be induced by inflammatory mediators such as IFN- $\gamma$ , enabling the proteasome to degrade non-ubiquitinated proteins [7, 14].

In adjuvant-induced arthritis model (AIA), as well as in other models of chronic inflammation, increased expression of E3 ubiquitin ligases MAFbx/atrogen-1 (muscle atrophy F-box) and MuRF-1 (muscle-specific RING finger protein 1) were observed in skeletal muscles [15, 16]. Additionally, a model of immobilization detected a higher expression of MuRF-1 in skeletal muscles [17, 18]. During inflammatory state and high exposure to inflammatory cytokines [19], eukaryotic cells can replace the constitutive subunits of the proteasome ( $\beta 5$ ,  $\beta 1$ , and  $\beta 2$ ) for alternative enzymatic subunits ( $\beta 5i$  (Psm8),  $\beta 1i$  (Psm9) and  $\beta 2i$  (Psm10) [20, 21]. The complex formed with the alternative enzymatic subunits is called induced proteasome and has different properties, such as

generating antigenic material for the major histocompatibility complex class I (MHC-I) [22].

The proteasome is an indispensable system for cell survival and plays a pivotal role in inflammatory and immune responses. In this context, increased proteasome-related proteins were identified circulating in patients' serum [23, 24]. Also, the proteasome activity was correlated with disease severity and immunologic activity [23, 24]. Immunosuppressive drugs like methotrexate (MTX) and TNF inhibitors (TNFi) are effective in treating RA by improving signs and symptoms of the disease and preventing joint damage [25, 26]. However, their effects on muscle wasting and on the proteasome system activity are unknown.

Therefore, this study evaluated the activity of muscle proteasome system in collagen-induced arthritis (CIA) and the effects of etanercept treatment compared to methotrexate treatment. Here, we show that the proteasome system presented alterations in CIA muscle and that the treatment by ETN was able to reduce this alteration.

## Materials and methods

### Animals and experimental groups

Male DBA/1 J mice aged 8 to 12 weeks were used. The animals were kept in 12-h light–dark cycles with free access to food and water. The mice were divided into four groups: CIA mice treated with saline (CIA-Vehicle,  $n=8$ ), CIA mice treated with etanercept (CIA-ETN,  $n=8$ ), CIA mice treated with methotrexate (CIA-MTX,  $n=8$ ), and healthy mice (CO,  $n=8$ ). The animals were randomized into each group using the website <http://www.graphpad.com/> (GraphPad Software, La Jolla, CA, USA). All in vivo and molecular analyses were performed by blinded researchers. This study followed the Guiding Principles for Research Involving Animals (NAS), and was approved by the Research Ethics Committee of the Hospital de Clínicas de Porto Alegre (protocol no. 2015-0286).

### Induction of CIA

Arthritis induction was performed using bovine type II collagen (CII; Chondrex Inc., Redmond, WA, USA; 2 mg mL<sup>-1</sup>) dissolved in 0.1-M acetic acid at 4 °C for 12 h and in Complete Freund's Adjuvant (CFA; Sigma, St Louis, USA; 2 mg mL<sup>-1</sup>) containing inactivated *Mycobacterium tuberculosis*. The emulsion (50  $\mu$ L of CII + CFA) was injected intradermally at the base of the tail on day 0. Moreover, the animals received a reinforcement of CII emulsified with incomplete Freund's adjuvant (without *M. tuberculosis*) in another site of the tail (booster injection) on day 18 [27]. During the procedures, the mice were anesthetized with isoflurane 10% (Abbott Laboratórios do Brasil Ltda., Brazil) and 90% oxygen. Healthy

control mice were manipulated and anesthetized during this period [28]. Animals were euthanized on day 45 by cervical dislocation after an isoflurane overdose. Gastrocnemius (GA) and tibialis anterior (TA) muscles were dissected and weighed after euthanasia, immediately frozen in liquid nitrogen, and stored at  $-80^{\circ}\text{C}$  for further analyses.

#### Clinical severity and measurement of edema

Arthritis severity was clinically determined for each paw, three times per week, according to a scale of 0 to 4 (0: no evidence of erythema and swelling; 1: erythema and mild swelling confined to the tarsals or metatarsals; 2: erythema and moderate swelling of tarsal and the metatarsal or tarsal and ankle joints; 3: erythema and severe swelling from the ankle to metatarsal joints; and 4: erythema and severe swelling encompassing the ankle, foot, and digits, or ankylosis of the limb) [29]. Clinical score, the sum of the four paws, can achieve a maximum score of 16. Hind paw edema was evaluated by latero-lateral measure of the mice hind paws with digital calipers (Myoto). The measurements were obtained at the time of the booster (18 days) and three times per week.

#### Drug treatment

Treatments started one week after booster injection and were administered intraperitoneally (IP) twice per week for six weeks. Etanercept (50 mg/ml Enbrel, Pfizer, New York, NY, EUA) and methotrexate (25 mg/ml Lexato, Laboratório Pierre Fabre do Brasil Ltda, Arcal, RJ, Brazil) were purchased. Etanercept (5.5 mg/kg) and methotrexate (35 mg/kg) were diluted in sterile saline solution (NaCl 0.9%) and maintained cold and in the dark until 10 min before the injections. The dosage used in this study was based on rodent models' treatment with both drugs [30, 31].

#### Animal body weight and muscle weight and joint histological score system

The animals were weighed once per week from day 0 to the end of experimentation. The difference of animal body weight during the experimental period was estimated ( $\Delta$  weight) considering the weight at induction time as baseline (day 0). Muscle weight was normalized with total body weight (mg/g) to analyze muscle proportion. The histological score system was applied by a blinded pathologist to evaluate individual joints and measure arthritis severity as previously described [28].

#### Determination of proteasome activity

To determine 26S proteasome activity, GA muscle was homogenized in 50 mM Tris-HCl pH 7.4, 150 mM NaCl, 5 mM MgCl<sub>2</sub>, 1 mM ethylenediaminetetra acetic

acid (EDTA), 250 mM sucrose, 0.1% Triton X-100 for 20S proteasome activity, and added 5 mM ATP and 1 mM dithiothreitol (DTT). Sample protein concentration was measured using the Pierce BCA Protein Assay Kit (Rockford, IL, USA). Fluorogenic peptide hydrolysis by 26S and 20S proteasomes were measured with muscle tissue homogenate. First, 30  $\mu\text{g}$  of the sample were pre-incubated with 26S assay buffer (50 mM Tris-HCl pH 7.4, 40 mM KCl, 5 mM MgCl<sub>2</sub>, 5 mM ATP, 0.5 mM DTT, 0.5 mg/ml BSA) or 20S assay buffer (25 mM HEPES pH 7.4, 0.5 mM EDTA, 0.03% SDS) with or without the specific inhibitors, 50 nM bortezomib (chymotrypsin-like activity, LKT-B5871, Enzo Life Sciences, Lausen, Switzerland) or 40  $\mu\text{M}$  Z-Pro-Nle-Asp-CHO (caspase-like activity, BML-ZW9490, Enzo Life Sciences, Lausen, Switzerland), for 30 min at  $37^{\circ}\text{C}$ . Afterward, substrate (final concentration 100  $\mu\text{M}$ ) was added to the chymotrypsin-like activity (Z-GGL-AMC, BML-ZW8505, Enzo Life Sciences, Lausen, Switzerland) or caspase-like activity (Z-LLE-MCA, BML-ZW9345, Enzo Life Sciences, Lausen, Switzerland). After 120 min of incubation at  $37^{\circ}\text{C}$ , the enzymatic reaction was measured at 355 nm excitation and 460 nm emission [13, 23]. Proteasome activity was considered as the difference between the activity with and without the specific inhibitor and was normalized using the results of CO animals, considered to have 100% activity.

#### mRNA and protein extraction

Total RNA from GA and TA muscles was isolated using the NucleoSpin<sup>®</sup> RNA/Protein kit (Macherey-Nagel, Düren, Germany). Muscle homogenates were placed into the NucleoSpin<sup>®</sup> RNA/Protein column, where RNA and DNA were bound to the silica membrane, and protein remained in the flow-through. NanoDrop 1000 Spectrophotometer (Thermo Scientific, Schwerte, Germany) was used to control quality and quantity of RNA and flow-through was used to isolate proteins from muscle tissues. Protein isolation proceeded following manufacturer' instructions, with a re-suspension in RIPA (Radioimmunoprecipitation assay buffer) composed of 50 mM Tris-HCl pH 7.4, 1% Triton x-100, 150 mM NaCl, 0.5% sodium deoxycholate, 2 mM EDTA, 50 mM NaF, 1 mM DTT, 2% SDS. Sample protein concentration was measured using the Pierce BCA Protein Assay Kit (Rockford, IL, USA). Isolated proteins were used to perform immunoblot analysis.

#### Real-time RT-PCR

Super Script<sup>™</sup> III First-Strand Synthesis System for real-time RT-PCR (Invitrogen, Karlsruhe, Germany) was used according to the manufacturer's instructions to synthesize first-strand cDNA from total RNA. Forward and

reverse primers of proteasome subunits Psma4, Psmb6, Psmb7, Psmb8, Psmb9, Psmb10, Rsp20, Ppia and HPRT1 for real-time RT-PCR were designed using the Primer3 program (Additional file 1: Table S1).

Real-time PCR was performed in triplicates using StepOne Plus Real-Time PCR (Applied Biosystems, Foster City, CA, USA), and mRNA of Rsp20, Ppia, and HPRT1 housekeeping genes were analyzed. Thus, HPRT1 were shown to be stable in the muscle and thus they were used to normalize mice muscle tissues. Differences in the relative expression between target and housekeeping genes were determined using the equation  $R = ECT \text{ housekeeping gene} / ECT \text{ target gene}$ , according to Pfaffl et al. [24].

### Western blot

Protein extracts (25  $\mu\text{g}$  per muscle) were separated by sodium dodecyl sulfate–polyacrylamide gel electrophoresis (SDS-PAGE) 12% and transferred to a polyvinylidene fluoride (PVDF) membrane, in which the remaining binding sites were blocked with 5% skim milk in tris buffer saline (TBS) pH 7.4. Then, membranes were incubated overnight with the following antibodies: anti- $\beta 5$  (1:2000, Ab3330, Abcam, Cambridge, England); anti- $\beta 1$  (1:1000, sc-100455, Santa Cruz Biotechnology, Dallas, TX, USA); anti- $\beta 5i$  (1:5000, Ab180606, Abcam, Cambridge, England); anti- $\beta 1i$  (1:300, sc-373689, Santa Cruz Biotechnology, Dallas, TX, USA); and anti-GAPDH (1:1000, sc-25778, Santa Cruz Biotechnology, Dallas, TX, USA). Detection was accomplished with anti-IgG antibodies coupled with horseradish peroxidase antibodies (1:1000; Dako, Denmark) and visualized by enhanced electrochemiluminescence Pierce ECL Western Blotting Substrate (Thermo Scientific, USA). Quantification on Western blot image was performed with the integrated density function of ImageJ (Bethesda, MD, USA) [21]. Proteasome subunits expression was normalized with CO animals, considered as 100% expression.

### Statistical analysis

Sample size was based on our group's previous research [28]. The results are expressed as mean values with standard error of the mean (SEM). The quantitative data were compared by one-way analysis of variance (ANOVA) followed by Tukey's test, and two-way ANOVA followed by Tukey's test. The histological score was compared among groups using the Kruskal–Wallis test, followed by Dunn's Multiple Comparison Test.  $p < 0.05$  was considered

significant. Values were analyzed using the statistical package GraphPad Prism 6 (GraphPad Software, La Jolla, CA, USA).

## Results

### Treatment with etanercept and methotrexate decreased hind paw swelling and clinical score in arthritic mice

CIA animals developed arthritis as expected, and the severity increased gradually over time. All arthritic mice reached the maximum clinical score seven weeks after the booster injection (Additional file 2: Fig. S1A, Fig. 1D). We observed a similar pattern in hind paw swelling, as CIA-Vehicle presented a gradual increase in hind paw diameter (Additional file 2: Fig. S1B). On day 26 after booster injection, CIA-Vehicle group reached the highest hind paw swelling and afterwards, with the presence of ankylosis, the edema gradually decreased (Additional file 2: Fig. S1B). The treatment with etanercept or methotrexate hindered the disease development, as lower clinical scores could be observed in the treated groups compared to CIA-Vehicle (Additional file 2: Fig. S1A, B,  $p$ : 0.0001 and  $p$ : 0.025, respectively). However, CIA-MTX group had increased clinical scores compared to CIA-ETN from days 28 to 36. Hind paw edema was significantly different between CIA-Vehicle- and CIA-ETN-treated mice from days 11 to 22 as well as CIA-MTX, from days 7 to 16 (Additional file 2: Fig. S1B,  $p$ : 0.008 and  $p$ : 0.033, respectively). After day 27, hind paw sizes did not differ among groups as paw edema decreased and cartilage erosion and joint damage ensued.

The joint histologic architecture was highly abnormal in CIA-Vehicle mice (Additional file 2: Fig. S1C, Fig. 1D), with pronounced inflammatory infiltrate and bone and cartilage erosion. In contrast, both CIA-MTX- and CIA-ETN-treated mice (Additional file 2: Fig. S1C) showed lower histological scores compared to CIA-Vehicle animals. However, only the CIA-ETN-treated animals preserved joint architecture to near normality, with significantly diminished cartilage and bone erosion, as well as pannus formation (Additional file 2: Fig. S1C).

### Etanercept treatment led to greater muscle weight compared to methotrexate treatment

The development of arthritis prevented weight gain in mice, which occurs in healthy conditions. However, from the fifth week, CIA-MTX had a significant decrease in weight compared to CIA-ETN group (Fig. 1A;  $p$ : 0.022).

(See figure on next page.)

**Fig. 1** Etanercept treatment increases muscle weight of mice compared to CIA-MTX and CIA-Vehicle groups. **A** Animal body weight and; **B**  $\Delta$  body weight, consisting of the difference of body weight values between the induction of arthritis and the end of the experiment; **C** GA and; **E** TA muscle weights (mg); **D–F** normalized by animal body weight at the end of the experimental period. CIA-Vehicle: CIA with PBS; CIA-ETN: CIA treated with etanercept; CIA-MTX: CIA treated with methotrexate. 400  $\times$  zoom, scale bar: 200  $\mu\text{m}$ . Data were analyzed by one-way ANOVA followed by Tukey's test and are presented as mean  $\pm$  SEM;  $n = 8$  animals per group. \* $p < 0.05$ ; \*\* $p < 0.01$

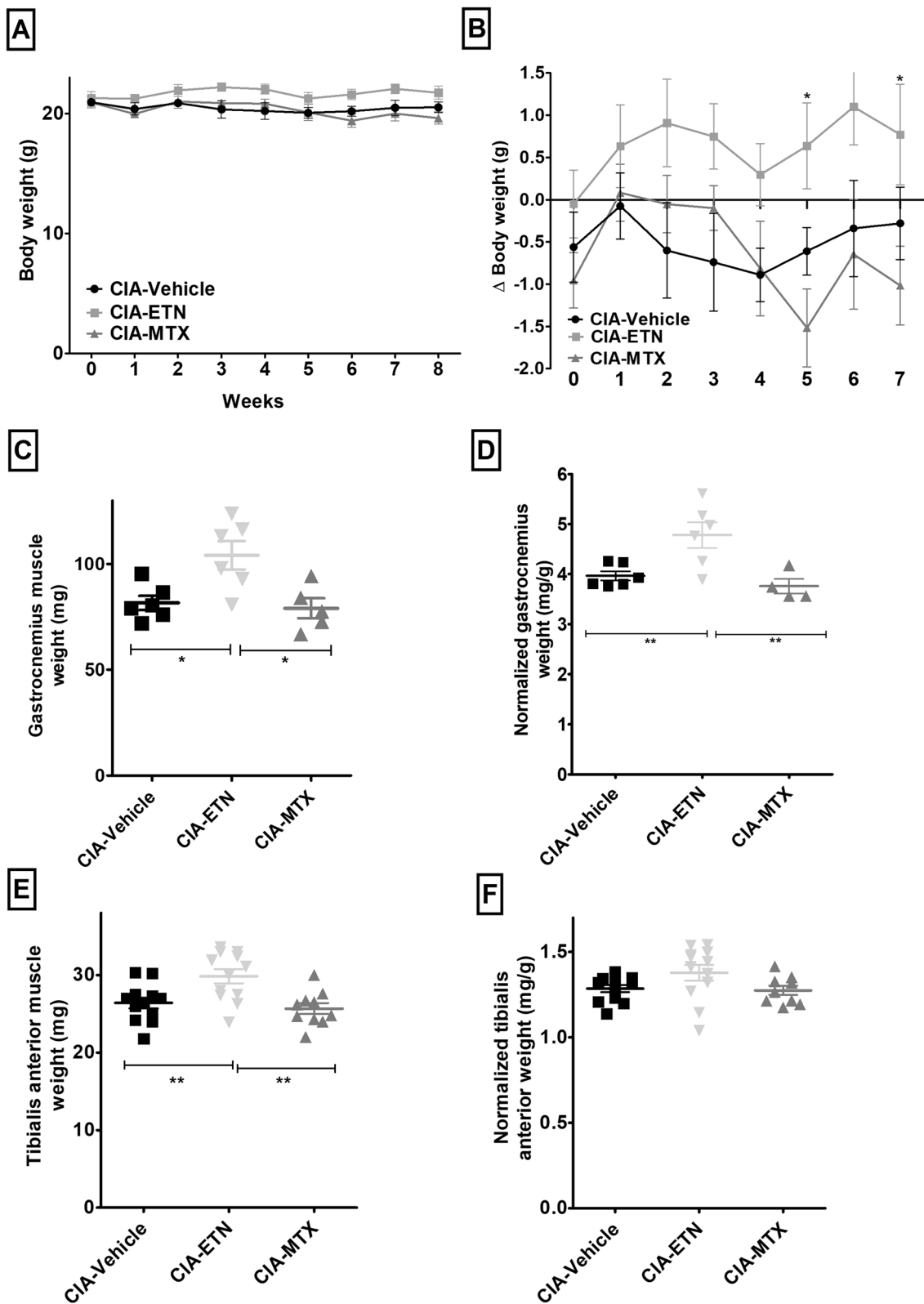


**Fig. 1** (See legend on previous page.)

Considering the normalized body weight at the induction of arthritis, CIA-ETN mice showed slight weight gain during the whole experimental period, whereas CIA-Vehicle and CIA-MTX mice lost weight. On weeks 5 and 7, CIA-ETN mice showed significantly greater body weight than CIA-MTX (Fig. 1B). GA and TA muscles showed greater weights in CIA-ETN mice compared to both CIA-Vehicle and CIA-MTX groups at the end of the experimental period (Fig. 1C–E,  $p$ : 0.0129,  $p$ : 0.0068, respectively). After normalization by body weight, GA muscle weight was still higher in CIA-ETN mice than

other groups (Fig. 1D–F,  $p$ : 0.013). (Fig. 1C–E,  $p$ : 0.012,  $p$ : 0.0068, respectively).

#### 26S caspase-like activity was reduced in muscles after etanercept treatment

The 26S chymotrypsin-like activity in GA muscle did not differ among groups (Fig. 2B). The percentage of 26S caspase-like activity was elevated in CIA-Vehicle and CIA-MTX groups compared to CO group (Fig. 2B,  $p$ : 0.0230,  $p$ : 0.005). CIA-ETN group presented attenuated 26S caspase-like activity, similar to the activity in CO group

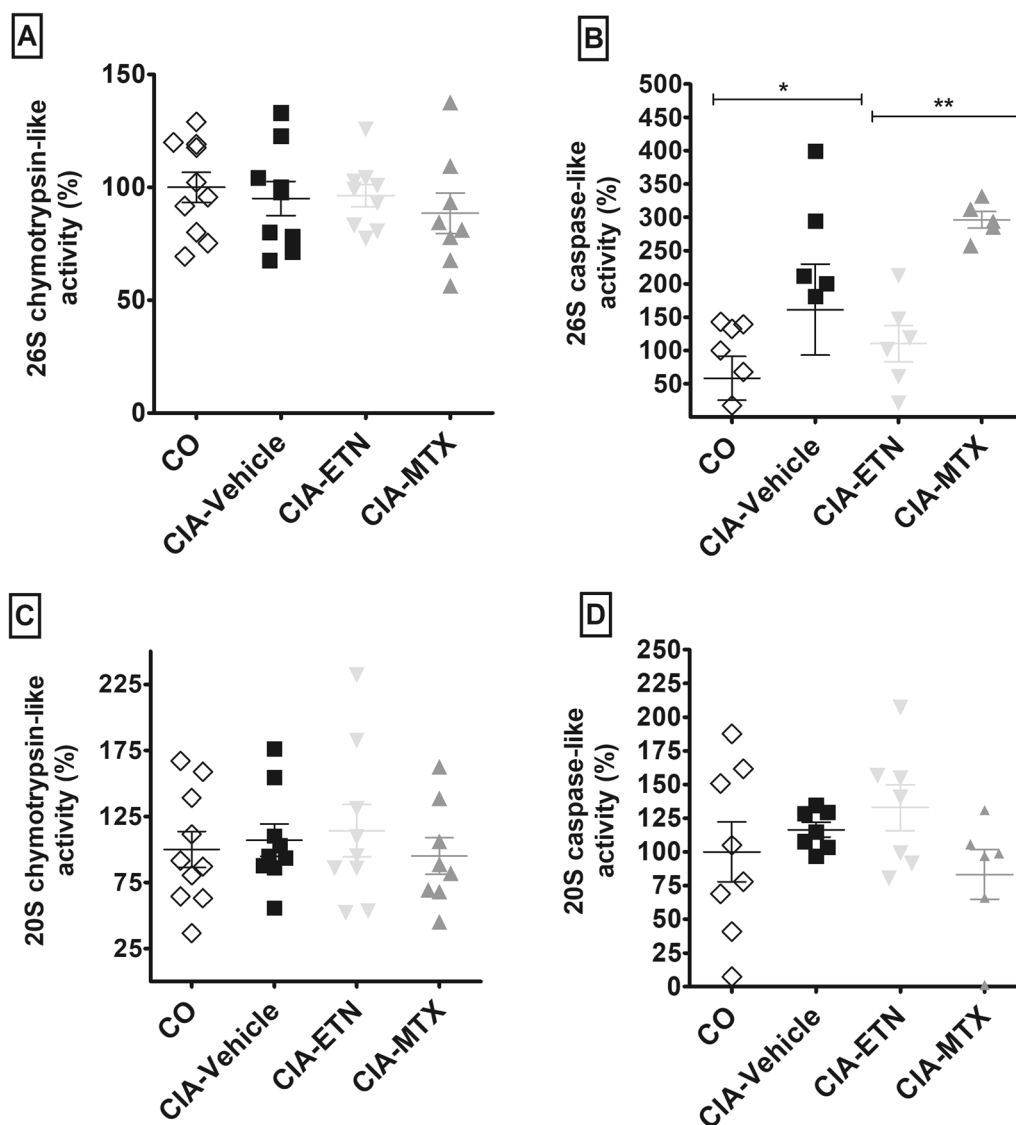


**Fig. 2** Etanercept treatment decreases 26S caspase-like activity compared to CIA-Vehicle and CIA-MTX groups. Proteasome activity was evaluated in GA muscle homogenates of arthritic and healthy animals, with specific inhibitors and fluorogenic substrates for chymotrypsin-like and caspase-like activity (A, B) for 26S and (C, D) 20S proteasomes. Activity is presented in % against values of CO group. CIA-Vehicle: CIA with PBS; CIA-ETN: CIA treated with etanercept; CIA-MTX: CIA treated with methotrexate. Data were analyzed by one-way ANOVA followed by Tukey's test and are presented as mean  $\pm$  SEM;  $n$  = 8 animals per group. \* $p$  < 0.05; \*\* $p$  < 0.01

(Fig. 2B), and significantly decreased compared to CIA-MTX group (Fig. 2B;  $p$ : 0.0057). We observed no significant differences among groups for chymotrypsin-like and caspase-like activities regarding 20S subunit activity (Fig. 2C, D).

**Proteasome-related gene expression levels were affected by etanercept and methotrexate treatments**

The mRNA expression of subunits PSM $\beta$ 8 and PSM $\beta$ 9 increased in muscles of CIA-MTX and CIA-Vehicle groups compared to CO group (Fig. 3C;  $p$ : 0.021,  $p$ : 0.039) (Fig. 3E;  $p$ : 0.001,  $p$ : 0.017, respectively, whereas CIA-Vehicle and CIA-MTX groups had decreased PSM $\beta$ 6 mRNA levels compared to CO group (Fig. 3D,  $p$ : 0.007,  $p$ : 0.017 respectively). PSM $\beta$ 5 (Fig. 3B), PSM $\alpha$ 4, PSM $\beta$ 7, and PSM $\beta$ 10 expressions did not show differences among groups (Additional file 2: Fig. S2). Moreover, we investigated the ubiquitin-ligase MuRF-1 mRNA levels to assess the activation of ubiquitin–proteasome

system. CIA-ETN presented a decrease in MuRF-1 mRNA expression compared to CIA-Vehicle and CO groups (Fig. 3A;  $p$ : 0.002,  $p$ : 0.007; respectively). CIA-MTX group also presented a decrease in MuRF-1 mRNA expression compared to CO group ( $p$ : 0.036); meanwhile, differences between CIA-Vehicle and CIA-MTX almost reached significance (Fig. 3;  $p$ : 0.06).

**Protein expression of proteasome subunits is altered in arthritic mice and treatments with etanercept and methotrexate restored these changes to a level similar to that of healthy mice**

The protein expression of proteasome subunits was altered in muscle of arthritic mice. The disease induced a decrease in PSM $\beta$ 5 expression, as observed when CIA-Vehicle group is compared to CO group (Fig. 4A;  $p$ : 0.0469). When we analyzed the CIA-ETN and CIA-MTX groups, both treatments increased PSM $\beta$ 5 subunit, similarly to CO group (Fig. 4A,  $p$ : 0.0025,  $p$ : 0.001,

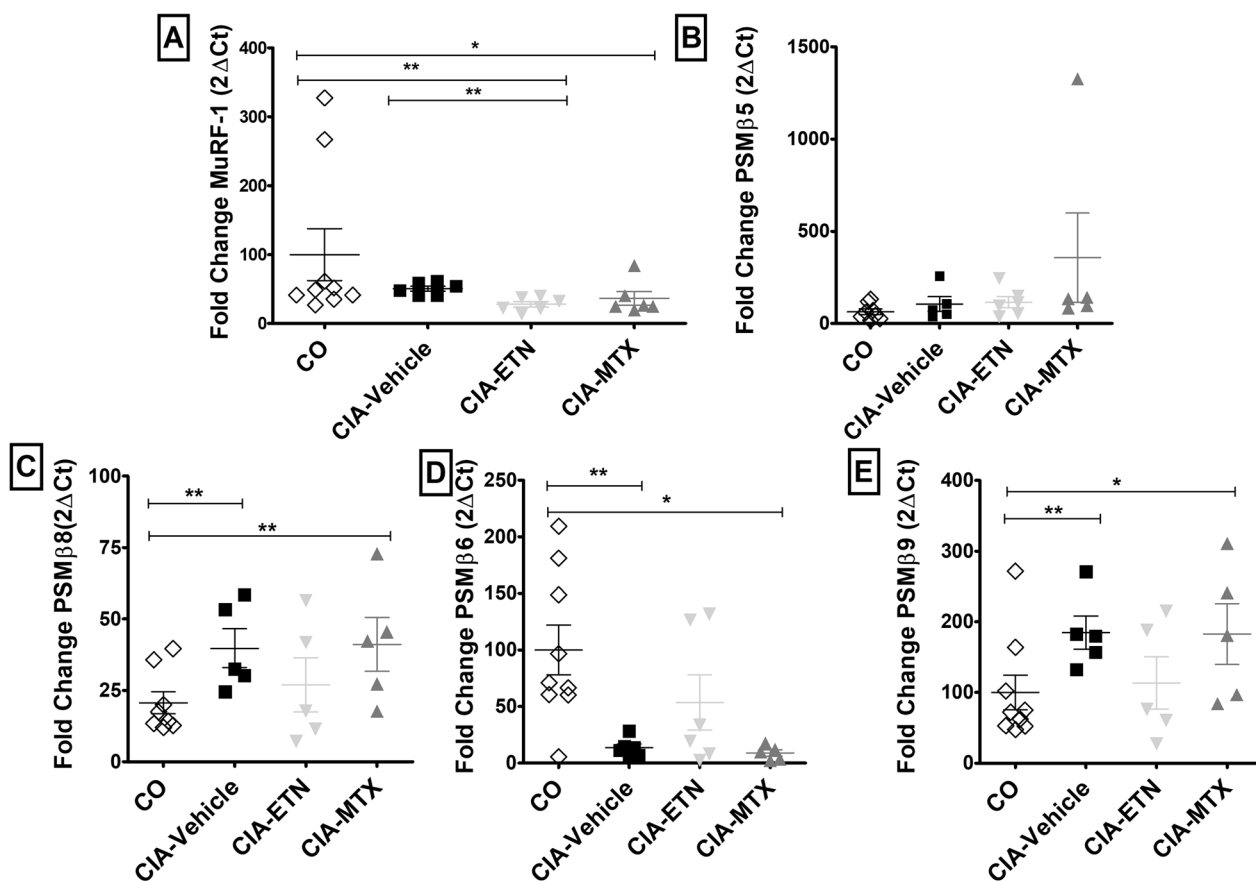


**Fig. 3** Proteasome-related gene expression levels were modulated by etanercept and methotrexate treatments. GA muscles of arthritic and healthy animals were used to extract mRNA and perform qRT-PCR for detection of **A** MuRF-1, **B** PSM $\beta$ 5, **C** PSM $\beta$ 8, **D** PSM $\beta$ 6, **E** PSM $\beta$ 9 subunits, and HPRT1 housekeeping gene. The mRNA expression is presented in fold change 2 $\Delta$ Ct versus values of CO group. CIA-Vehicle: CIA with PBS; CIA-ETN: CIA treated with etanercept; CIA-MTX: CIA treated with methotrexate. Data were analyzed by one-way ANOVA followed by Tukey’s test and are presented as mean  $\pm$  SEM; n = 7 animals per group. \* $p$  < 0.05; \*\* $p$  < 0.01

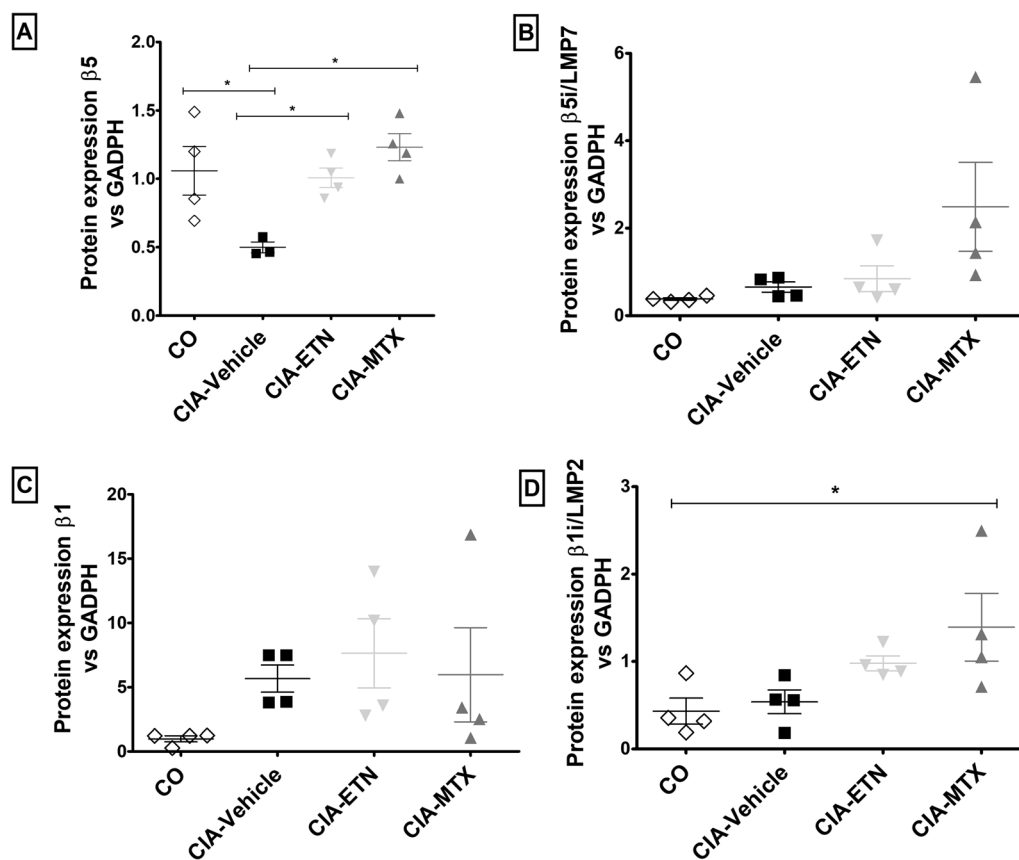


**Fig. 4** Treatments with etanercept and methotrexate reverse changes in proteasome subunits protein expression levels. GA muscle homogenates of arthritic and healthy animals were used for protein detection of **A** PSMβ5, **B** PSMβ5-induced, **C** PSMβ1, **D** PSMβ1-induced, and GAPDH by Western blot images. Protein levels are presented in % versus values of CO group. CIA-Vehicle: CIA with PBS; CIA-ETN: CIA treated with etanercept; CIA-MTX: CIA treated with methotrexate. Data were analyzed by one-way ANOVA followed by Tukey's test and are presented as mean ± SEM; n = 8 animals per group. \* $p < 0.05$ ; \*\* $p < 0.01$

respectively). Moreover, this study analyzed subunits induced by inflammation; the β5 (LMP7) induced subunit did not present alterations among groups (Fig. 4B), whereas the induced subunit β1 (LMP2) was enhanced in CIA-MTX group compared to CO group (Fig. 4D;  $p$ : 0.043). No changes were detected in PSMβ1 expression (Fig. 4C).

## Discussion

Little is known about the development mechanisms of muscle wasting in RA and the impact of the most used anti-rheumatic drugs, such as methotrexate and anti-TNFs on muscle mass. Our study confirmed that the muscle loss associated with the CIA model could be modulated differentially by the treatments tested—methotrexate and etanercept—as determined by muscle weight and proteasome activity and subunit expression.

As expected, both treatments alleviated clinical aspects in the CIA model, in line with previous reports [32, 33]. The CIA-ETN group presented stable body

weight and slight muscle weight gain over time compared to CIA-MTX and CIA-vehicle groups, whereas no differences were found between CIA-MTX and CIA-vehicle groups. Marcora et al. compared methotrexate versus etanercept therapies in 26 RA patients and did not observe significant changes in body composition [34]. However, the patients who gained weight (> 3%) in their baseline and body mass over the 24-week follow-up period (6/treatment group) were using etanercept as a primordial treatment. Moreover, a greater proportion of fat-free mass was found in etanercept use when compared with methotrexate use, whereas no difference on fat mass was observed [34]. Corroborating with this data, Engvall et al. showed an increase in lean body mass in early RA patients using infliximab (TNF-inhibitor) compared to methotrexate use [34, 35]. This result may be explained by the strong effects of TNF on skeletal muscle, such as accelerated catabolism, disrupted contractile dysfunction and impaired myogenesis [23, 36].



We further studied the activation of cellular systems possibly involved in protein breakdown in muscle cells, like the proteasome system. Previous data of our group indicated rising levels of MurF-1 expression in the CIA model (not published). MurF-1 is an E3 ligase protein highly active in the presence of aberrant proteins. MurF-1 increases gene expression via polyubiquitination and degradation of transcription factors related to rises in the proteasome catalytic chamber 20S (20S proteasome) [14]. In this study, we confirmed alterations in gene expression related to MurF-1. We found a decrease in MurF-1 mRNA expression when arthritic mice were subjected to etanercept therapy, which could be explained as a decrease in proteasome activity [37–39]. However, CIA-vehicle and CO groups presented similar levels of MurF-1. High levels of systemic TNF can induce atrophic signaling by upregulating the transcription of ubiquitin ligases MAFbx (atrogin-1) and MuRF1 [40, 41]. Thus, TNF-induced loss of skeletal muscle contractility requires MuRF1 induction, explaining the role of MurF-1 in loss of muscle mass and function by activating protein breakdown systems and potential muscle atrophy markers [9, 42].

The proteasome system is a multicompartiment system for degradation of ubiquitinated proteins and may be modulated during an inflammatory state [43, 44]. The 26S proteasome involves multiple enzymatic and non-enzymatic steps, including the binding of ubiquitinated substrates to the 19S, opening the gated channel into the 20S for proteolysis [37, 43]. We found that in the skeletal muscles of arthritic mice 26S proteasome has a high caspase-like activity and a reduction in caspase-like activity without changes in chymotrypsin-like activity after treatment with etanercept. Proteasome-specific changes are elicited by exposure to proinflammatory cytokines such as TNF and IL-6, which may induce  $\beta$ -subunits to perform proteolytic activities, such as caspase-like ( $\beta$ 1 subunits) and chymotrypsin-like ( $\beta$ 5 subunits) [3, 44–46]. Besides, we observed a higher caspase-like activity in 26S proteasome, whereas the 20S proteasome remained unchanged. As 26S proteasome contemplate both 19S and 20S proteasomes, the changes we observed are reminiscent of a larger activation of the proteasome system since the beginning of the inflammatory process in the CIA model.

Proteasome-related gene expression increases when the traffic of protein breakdown demands higher proteolysis activity from the proteasome system [43, 47]. Our study shows that the CIA model altered the expression of proteasome subunits (lower PSM $\beta$ 6 and higher PSM $\beta$ 9, PSM $\beta$ 8) and was associated with muscle wasting of chronic experimental arthritis model. Thus, CIA-MTX mice presented improvement of the disease clinical

characteristics without alterations in muscle wasting, whereas CIA-ETN mice presented less muscle loss.

The etanercept treatment seems to modulate the proteasome system at a genetic level by matching the PSM $\beta$ 8, PSM $\beta$ 6, and PSM $\beta$ 9 levels to the CO group. However, this could be reflected by an increase in PSM $\beta$ 9 ( $\beta$ 1i) and a decrease in PSM $\beta$ 6 ( $\beta$ 1) expression in CIA muscles. In patients with idiopathic inflammatory myositis, upregulation of PSM $\beta$ 8 and PSM $\beta$ 9 was detected in muscle biopsies as well as changes related to inflammatory infiltration [48]. Since inducible proteasome subunits have a different enzymatic activity [49, 50], our findings could explain the difference in proteasome caspase-like activity. These results indicates that muscle wasting in experimental arthritis may be related to  $\beta$ 1i subunit expression and activity, associated with enhanced disease activity and induction of immunoproteasome subunits in CIA muscle. When exposed to pro-inflammatory cytokines, such as TNF- $\alpha$  and IFN- $\gamma$  [51], eukaryotic cells express different subunits,  $\beta$ 1i,  $\beta$ 2i, and  $\beta$ 5i, which are included in the proteasome replacing the constitutive subunits during neosynthesis [10, 20]. PSM $\beta$ 9 ( $\beta$ 1i) and PSM $\beta$ 8 ( $\beta$ 2i) are transcribed into proteins when the constitutive subunits have been replaced with a more efficient action of the proteasome system [50, 52]. We hypothesized that the pro-inflammatory state triggers muscle loss by high gene expression of induced subunits of 26S proteasome and influences the protein expression levels of the same subunits.

The inhibition of TNF in wasting diseases is described to decrease muscle wasting and proteasome activity and expression [44, 53]. Regarding MTX treatment, the clinical features and disease progression were improved, however MTX administration does not have a significant role in muscle wasting in the CIA model. Thus, TNF-induced alterations in the proteasome pathway, and apparently TNF inhibitors seem to have a role in preventing muscle atrophy due to inflammation. Some of this study's limitations were the lack of intracellular markers that may be involved in the activation of the proteasome system and the early state of muscle wasting in the CIA model.

## Conclusion

We found enhanced proteasome activity (caspase-like activity) and increased PSM $\beta$ 8 and PSM $\beta$ 9 mRNA levels in CIA mice. Etanercept treatment was able to modulate proteasome so that its activity and gene expression were compared to CO after TNF inhibition. Anti-TNF treatment may be an interesting approach to attenuate the arthritis-related muscle wasting. As additional mechanisms besides TNF could be involved in muscle wasting of arthritis, further studies are necessary to explain the

## role of proteasome and the effects of TNF inhibition on muscle wasting in arthritis.

### Abbreviations

RA	Rheumatoid arthritis
TNF- $\alpha$	Tumor necrosis factor $\alpha$
IL-1 $\beta$	Interleukin 1 $\beta$
IL-6	Interleukin 6
TGF- $\beta$	Transforming growth factor $\beta$
MTX	Methotrexate
csDMARDs	Synthetic disease-modifying antirheumatic drugs
PI3K	Protein kinase B
IGF-1	Insulin-like growth factor-1
NF-K $\beta$	Factor nuclear kappa B
CIA	Collagen induced-arthritis
MurF-1	Muscle-specific ring finger protein-1
LC3	Microtubule-associated protein 1 light chain 3
Atg5	Autophagy related 5
p62	Sequestosome-1
CFA	Freund's complete adjuvant
CII	Bovine type II collagen
CIA-ETN	Treatment with etanercept
CIA-vehicle	Treatment with saline
TA	Tibialis anterior
GA	Gastrocnemius
HE	Hematoxylin and eosin
GAPDH	Gliceraldeido-3-fosfate-desidrogenase
PBS	Phosphate-buffered saline
S.E.M.	Standard error
ANOVA	Two-way analysis of variance
CSA	Cross-sectional area

### Supplementary Information

The online version contains supplementary material available at <https://doi.org/10.1186/s42358-023-00292-5>.

**Additional file 1. Table S1.** Primer sequences designed in Primer 3 software used for rt-PCR experiments from collagen-induced arthritis (CIA) mouse muscles.

**Additional file 2. Figure S1.** CIA mice develop AR as expected and ETN and MTX treatments were able to slow down disease development. Progression of arthritis was analyzed by **A** clinical score and **B** hind paw edema, through hind paw diameter, every two days from booster injection (day 0). **C** MTX-CIA and CIA-ETN mice demonstrated an improvement in joint histology. **D** Histopathology of normal joint of an animal not induced with CI; CIA-Vehicle mice with CIA showed infiltration of inflammatory cells with *pannus* formation and large cartilage and bone erosion; 1—Infiltration of inflammatory cells, 2—Cartilage erosion, 3—Bone erosion, 4—*Pannus*. Data is presented as mean  $\pm$  SEM from 8 animals each group. \* $p < 0.05$  versus MTX analyzed by two-way ANOVA followed by Bonferroni's test. **Figure S2.** mRNA expression from muscles of arthritic and healthy animals. GA muscle of animals was used to extract mRNA from muscle tissue, transform in cDNA and perform real-time RT-PCR for *Psmb7* (**A**), *Psmb10* (**B**) and *Psm4* (**C**) subunits, followed by normalization with housekeeping gene HPRT1. mRNA expression is presented in % versus CO values. CIA, Collagen-induced arthritis non-treated; ETN, CIA treated with etanercept; MTX, CIA treated with methotrexate; CO, Healthy control animals. Data is presented as mean  $\pm$  SEM from 7 animals in each group and was analyzed by one-way ANOVA followed by Turkey's test.

### Acknowledgements

We thank the Unidade de Experimentação Animal (Hospital de Clínicas de Porto Alegre) for their help during animal experimentation. The Coordination for the Improvement of Higher Education Personnel (CAPES) and the Rio Grande do Sul Research Foundation (FAPERGS) granted scholarships for students who helped develop this study. This study was supported by the

Research Incentive Fund (FIPE) of the Hospital de Clínicas de Porto Alegre and the National Council for Scientific and Technological Development (CNPq).

### Author contributions

VONT participated in every step of the experimentation; BJB participated in experimentation and writing; RES participated in writing; PVGA participated in study design, animal experimentation, and manuscript draft; KG participated in all proteasome assays and manuscript draft; JMSS participated in animal experimentation; LIF participated in study design and manuscript draft, FV performed joint histopathological analysis; LM-G participated in proteasome assays; EF provided orientation on proteasome analysis and participated in manuscript draft; RMX gave orientation and participated in study design and manuscript writing. All authors read and approved the final manuscript.

### Funding

This study was funded by the Research Incentive Fund of the Hospital de Clínicas de Porto Alegre (FIPE-HCPA) [No. 12-0044 and No. 15-0286].

### Availability of data and materials

The data used to support the findings of this study are included within the article.

### Declarations

#### Ethics approval and consent to participate

All experiments were performed according to the Guiding Principles for Research Involving Animals (NAS) and this study was approved by the Research Ethics Committee of the Hospital de Clínicas de Porto Alegre (protocol no. 2015-0286).

#### Consent for publication

Not applicable.

#### Competing interests

The authors declare that they have no competing interests.

#### Author details

<sup>1</sup>Medical Sciences Program, Medicine Department, Universidade Federal do Rio Grande do Sul, Porto Alegre, Brazil. <sup>2</sup>Laboratório de Doenças Autoimunes, Hospital de Clínicas de Porto Alegre, Ramiro Barcelos Street, Santa Cecília, Porto Alegre 2350, Brazil. <sup>3</sup>Schwerpunkt Rheumatologie und Klinische Immunologie, Charité-Universitätsmedizin Berlin, Berlin, Germany. <sup>4</sup>Health and Human Development Department, Universidade La Salle, Canoas, Brazil. <sup>5</sup>Patology Department, Faculdade de Odontologia, Universidade Federal do Rio Grande do Sul, Porto Alegre, Brazil. <sup>6</sup>University of California San Diego Medical Center Library, University of California San Diego School of Medicine, San Diego, USA.

Received: 31 January 2022 Accepted: 5 March 2023

Published online: 22 March 2023

### References

- Smolen JS, Aletaha D, Barton A, Burmester GR, Emery P, Firestein GS, et al. Rheumatoid arthritis. *Nat Rev Dis Prim* [Internet]. 2018 Feb 8 [cited 2021 Jan 13];4. Available from: <https://pubmed.ncbi.nlm.nih.gov/29417936/>
- Roubenoff R, Roubenoff RA, Ward LM, Holland SM, Hellmann DB. Rheumatoid cachexia: depletion of lean body mass in rheumatoid arthritis. Possible association with tumor necrosis factor. *J Rheumatol*. 1992;19(10):1505–10.
- Roubenoff R, Roubenoff RA, Cannon JG, Kehayias JJ, Zhuang H, Dawson-Hughes B, et al. Rheumatoid cachexia: cytokine-driven hypermetabolism accompanying reduced body cell mass in chronic inflammation. *J Clin Invest*. 1994;93(6):2379–86.
- Santo RC, Hein T, Xavier RM. The effect of pharmacological treatment on rheumatoid arthritis related sarcopenia: a integrative review. *Curr Rheumatol Res*. 2021;2:5–11.

5. Sakuma K, Yamaguchi A. Sarcopenia and cachexia: the adaptations of negative regulators of skeletal muscle mass. *J Cachexia Sarcopenia Muscle*. 2012;3(2):77–94.
6. Naujokat C, Fuchs D, Berges C. Adaptive modification and flexibility of the proteasome system in response to proteasome inhibition. *Biochim Biophys Acta*. 2007;1773(9):1389–97.
7. Huber EM, Groll M. Inhibitors for the immuno- and constitutive proteasome: current and future trends in drug development. *Angew Chem Int Ed Engl*. 2012;51(35):8708–20.
8. Wolf DH, Hilt W. The proteasome: a proteolytic nanomachine of cell regulation and waste disposal. *Biochim Biophys Acta*. 2004;1695(1–3):19–31.
9. Dondelinger Y, Darding M, Bertrand MJM, Walczak H. Poly-ubiquitination in TNFR1-mediated necroptosis. *Cell Mol Life Sci*. 2016;73:2165–76.
10. Aa K, Aa B. Proteasome: a nanomachinery of creative destruction. *Biochemistry (Mosc)*. 2019;84(Suppl 1):159–92.
11. Reboud-Ravaux M. The proteasome—structural aspects and inhibitors: a second life for a validated drug target. *Biol Aujourd'hui*. 2021;215(1–2):1–23.
12. Bard JA, Goodall EA, Greene ER, Jonsson E, Dong KC, Martin A. Structure and function of the 26S proteasome. *Annu Rev Biochem*. 2018;87:697–724.
13. Baumeister W, Walz J, Zühl F, Seemüller E. The proteasome: paradigm of a self-compartmentalizing protease. *Cell*. 1998;92(3):367–80.
14. Wu J. On the role of proteasomes in cell biology and proteasome inhibition as a novel frontier in the development of immunosuppressants. *Am J Transplant Off J Am Soc Transplant Am Soc Transpl Surg*. 2002;2(10):904–12.
15. Yannaki E, Papadopoulou A, Athanasiou E, Kaloyannidis P, Paraskeva A, Bougiouklis D, Palladas P, Yiangou M, Anagnostopoulos A. The proteasome inhibitor bortezomib drastically affects inflammation and bone disease in adjuvant-induced arthritis in rats. *Arthritis Rheum*. 2010;62(11):3277–88. <https://doi.org/10.1002/art.27690>.
16. Granado M, Martín AI, Priego T, López-Calderón A, Villanúa MA. Tumour necrosis factor blockade did not prevent the increase of muscular muscle RING finger-1 and muscle atrophy F-box in arthritic rats. *J Endocrinol*. 2006;191(1):319–26. <https://doi.org/10.1677/joe.1.06931>.
17. Caron AZ, Drouin G, Desrosiers J, Trensz F, Grenier G. A novel hindlimb immobilization procedure for studying skeletal muscle atrophy and recovery in mouse. *J Appl Physiol*. 2009;106(6):2049–59.
18. de Oliveira Nunes Teixeira V, Filippin LI, Viacava PR, de Oliveira PG, Xavier RM. Muscle wasting in collagen-induced arthritis and disuse atrophy. *Exp Biol Med*. 2013;238(12):1421–30.
19. Hallermalm K, Seki K, Wei C, Castelli C, Rivoltini L, Kiessling R, et al. Tumor necrosis factor- $\alpha$  induces coordinated changes in major histocompatibility class I presentation pathway, resulting in increased stability of class I complexes at the cell surface. *Blood*. 2001;98(4):1108–15.
20. Eleuteri AM, Kohanski RA, Cardozo C, Orlowski M. Bovine spleen multicatalytic proteinase complex (proteasome). Replacement of X, Y, and Z subunits by LMP7, LMP2, and MECL1 and changes in properties and specificity. *J Biol Chem*. 1997;272(18):11824–31.
21. Ustrell V, Pratt G, Rechsteiner M. Effects of interferon gamma and major histocompatibility complex-encoded subunits on peptidase activities of human multicatalytic proteases. *Proc Natl Acad Sci U S A*. 1995;92(2):584–8.
22. Goetzke CC, Ebstain F, Kallinich T. Role of proteasomes in inflammation. *J Clin Med*. 2021;10(8):1783.
23. Zoeger A, Blau M, Egerer K, Feist E, Dahlmann B. Circulating proteasomes are functional and have a subtype pattern distinct from 20S proteasomes in major blood cells. *Clin Chem*. 2006;52(11):2079–86.
24. Egerer K, Kuckelkorn U, Rudolph PE, Rückert JC, Dörner T, Burmester G-R, et al. Circulating proteasomes are markers of cell damage and immunologic activity in autoimmune diseases. *J Rheumatol*. 2002;29(10):2045–52.
25. Link T, Kepner A, Coruso O, Dilip M, Jacobson R, Stanovski L. Role of tumor necrosis factor- $\alpha$  in rheumatoid arthritis. *FASEB J*. 2018;32(1):817–12.
26. Abbott JD, Moreland LW. Rheumatoid arthritis: developing pharmacological therapies. *Expert Opin Investig Drugs*. 2004;13(8):1007–18.
27. Oliveira-Freitas VL, Thomaz LDGR, Simoneti LEL, Malfitano C, De Angelis K, Ulbrich JM, et al. RC-3095, a selective gastrin-releasing peptide receptor antagonist, does not protect the lungs in an experimental model of lung ischemia-reperfusion injury. *Biomed Res Int*. 2015;2015:1–7.
28. Filippin LI, Teixeira VN, Viacava PR, Lora PS, Xavier LL, Xavier RM. Temporal development of muscle atrophy in murine model of arthritis is related to disease severity. *J Cachexia Sarcopenia Muscle*. 2013;4(3):231–8.
29. Oliveira PG, Grespan R, Pinto LG, Meurer L, Brenol JCT, Roesler R, et al. Protective effect of RC-3095, an antagonist of the gastrin-releasing peptide receptor, in experimental arthritis. *Arthritis Rheum*. 2011;63(10):2956–65.
30. Kerwar SS, Oronsky AL. Methotrexate in rheumatoid arthritis: studies with animal models. *Adv Enzyme Regul*. 1989;29:247–65. [https://doi.org/10.1016/0065-2571\(89\)90105-2](https://doi.org/10.1016/0065-2571(89)90105-2).
31. Lon HK, Liu D, Zhang Q, DuBois DC, Almon RR, Jusko WJ. Pharmacokinetic-pharmacodynamic disease progression model for effect of etanercept in Lewis rats with collagen-induced arthritis. *Pharm Res*. 2011;28(7):1622–30. <https://doi.org/10.1007/s11095-011-0396-7>.
32. Castellero E, Martín AI, López-Menduiña M, Granado M, Villanúa MÁ, López-Calderón A. IGF-I system, atrogenes and myogenic regulatory factors in arthritis induced muscle wasting. *Mol Cell Endocrinol*. 2009;309(1–2):8–16.
33. Ibañez De Cáceres I, Villanúa MA, Soto L, Martín AI, López-Calderón A. IGF-I and IGF-I-binding proteins in rats with adjuvant-induced arthritis given recombinant human growth hormone. *J Endocrinol*. 2000;165(3):537–44.
34. Randomized phase 2 trial of anti-tumor necrosis factor therapy for cachexia in patients with early rheumatoid arthritis—PubMed [Internet]. [cited 2020 Jun 25]. Available from: <https://pubmed.ncbi.nlm.nih.gov/17158431/>.
35. Engvall I-L, Tengstrand B, Brismar K, Hafström I. Infliximab therapy increases body fat mass in early rheumatoid arthritis independently of changes in disease activity and levels of leptin and adiponectin: a randomised study over 21 months. *Arthritis Res Ther*. 2010;12(5):R197.
36. Sasakawa T, Sasakawa Y, Ohkubo Y, Mutoh S. FK506 ameliorates spontaneous locomotor activity in collagen-induced arthritis: implication of distinct effect from suppression of inflammation. *Int Immunopharmacol*. 2005;5(3):503–10.
37. Aiken CT, Kaake RM, Wang X, Huang L. Oxidative stress-mediated regulation of proteasome complexes. *Mol Cell Proteomics*. 2011;10(5):R110.006924.
38. Filippin LI, Vercelino R, Marroni NP, Xavier RM. Redox signalling and the inflammatory response in rheumatoid arthritis [Internet]. Vol. 152, *Clinical and Experimental Immunology*. Clin Exp Immunol; 2008 [cited 2021 May 20]. p. 415–22. Available from: <https://pubmed.ncbi.nlm.nih.gov/18422737/>.
39. Yamada T, Place N, Kosterina N, Östberg T, Zhang SJ, Grundtman C, et al. Impaired myofibrillar function in the soleus muscle of mice with collagen-induced arthritis. *Arthritis Rheum*. 2009;60(11):3280–9.
40. Valentine RJ, Jefferson MA, Kohut ML, Eo H. Ixomax attenuates LPS-induced inflammation and MuRF1 expression in mouse skeletal muscle. *Physiol Rep*. 2018;6(23):e13941.
41. Adams V, Linke A, Gielen S, Erbs S, Hambrecht R, Schuler G. Modulation of MuRF-1 and MAFbx expression in the myocardium by physical exercise training. *Eur J Prev Cardiol*. 2008;15(3):293–9.
42. Li YP, Reid MB. NF- $\kappa$ B mediates the protein loss induced by TNF- $\alpha$  in differentiated skeletal muscle myotubes. *Am J Physiol Regul Integr Comp Physiol*. 2000;279(4):R1165–70.
43. Collins GA, Goldberg AL. The logic of the 26S proteasome, vol. 169. Cell Press; 2017. p. 792–806.
44. Ferrington DA, Husom AD, Thompson LV. Altered proteasome structure, function, and oxidation in aged muscle. *FASEB J*. 2005;19(6):1–24.
45. Jones BA, Riegsecker S, Rahman A, Beamer M, Aboulaiwi W, Khuder SA, et al. Role of ADAM-17, p38 MAPK, Cathepsins, and the proteasome pathway in the synthesis and shedding of fractalkine/CX3CL1 in rheumatoid arthritis. *Arthritis Rheum*. 2013;65(11):2814–25.
46. Glickman MH, Ciechanover A. The ubiquitin-proteasome proteolytic pathway: destruction for the sake of construction. *Physiol Rev*. 2002;82:373–428.
47. Jackman RW, Kandarian SC. The molecular basis of skeletal muscle atrophy. *Am J Physiol Cell Physiol*. 2004;287(4):C834–43.
48. Ghannam K, Martínez-Gamboa L, Spengler L, Krause S, Smiljanovic B, Bonin M, et al. Upregulation of immunoproteasome subunits in myositis indicates active inflammation with involvement of antigen presenting cells, CD8 T-cells and IFN $\gamma$ . *PLoS ONE*. 2014;9(8): 104048.

49. Tanaka K. The proteasome: overview of structure and functions. *Proc Jpn Acad Ser B Phys Biol Sci.* 2009;85:12–36.
50. Ferrington DA, Gregerson DS. Immunoproteasomes: structure, function, and antigen presentation. In: *Progress in molecular biology and translational science* [Internet]. Elsevier B.V.; 2012 [cited 2021 May 20]. p. 75–112. Available from: /pmc/articles/PMC4405001/
51. Hallermalm K, Seki K, Wei C, Castelli C, Rivoltini L, Kiessling R, et al. Tumor necrosis factor- $\alpha$  induces coordinated changes in major histocompatibility class I presentation pathway, resulting in increased stability of class I complexes at the cell surface. *Blood.* 2001;98(4):1108–15.
52. Behl T, Chadha S, Sachdeva M, Kumar A, Hafeez A, Mehta V, et al. Ubiquitination in rheumatoid arthritis. *Life Sci.* 2020;261(July):118459.
53. Brown RA, Spina D, Butt S, Summers GD. Long-term effects of anti-tumour necrosis factor therapy on weight in patients with rheumatoid arthritis. *Clin Rheumatol.* 2012;31(3):455–61.

### Publisher's Note

Springer Nature remains neutral with regard to jurisdictional claims in published maps and institutional affiliations.

Ready to submit your research? Choose BMC and benefit from:

- fast, convenient online submission
- thorough peer review by experienced researchers in your field
- rapid publication on acceptance
- support for research data, including large and complex data types
- gold Open Access which fosters wider collaboration and increased citations
- maximum visibility for your research: over 100M website views per year

At BMC, research is always in progress.

Learn more [biomedcentral.com/submissions](https://biomedcentral.com/submissions)

